ARMY RESEARCH LABORATORY

Polyethylene-Based Polyurethane Copolymers and Block Copolymers

C.A. Byrne, C.R. Desper, N.S. Schneider,
B. Chu, and Y.J. Li

ARL-TR-649

November 1994

REPORT DOCUMENTATION PAGE

Form Approved
OMB No. 0704-0188

1. AGENCY USE ONLY *(Leave blank)*

2. REPORT DATE
November 1994

3. REPORT TYPE AND DATES COVERED
Final

4. TITLE AND SUBTITLE
Polyethylene-Based Polyurethane Copolymers and
Block Copolymers

5. FUNDING NUMBERS

6. AUTHOR(S)
C.A. Byrne, C.R. Desper, *N.S. Schneider,
**B. Chu, and Y.J. Li

7. PERFORMING ORGANIZATION NAME(S) AND ADDRESS(ES)
Army Research Laboratory
Watertown, MA 02172-0001
ATTN: AMSRL-MA-PB

8. PERFORMING ORGANIZATION REPORT NUMBER
ARL-TR-649

9. SPONSORING/MONITORING AGENCY NAME(S) AND ADDRESS(ES)

10. SPONSORING/MONITORING AGENCY REPORT NUMBER

11. SUPPLEMENTARY NOTES
*N.S. Schneider, Geocenters, Inc., 7 Wells Ave., Newton, MA 02159
**B. Chu and Y.J. Li, Dept. of Chemistry, State University of New York at Stony Brook, Stony Brook, NY 11794-3400

12a. DISTRIBUTION/AVAILABILITY STATEMENT
Approved for public release; distribution unlimited.

12b. DISTRIBUTION CODE

13. ABSTRACT *(Maximum 200 words)*

Low molecular weight hydroxy terminated polyethylene (HTPE) containing on average an ethyl group every 16-18 carbon atoms, and a hydroxy functionality of 2.6, has been used to prepare polyurethane copolymers and block copolymers which have good solvent resistance. The polymers show somewhat complicated thermal behavior, including T_g's at around -40°C due to the HTPE and diffuse endotherms between 40 and 60°C. The simple copolymers, containing only the polyol and a diisocyanate, show infrared evidence for two phases in the case where CHDI (trans-1,4-diisocyanatocyclohexane) was used, and poorer phase separation where other diisocyanates were used. Dynamic mechanical spectra show very broad tan delta transitions for the copolymers in the range of -9 to -23°C. All the polymers exhibit another transition in the G" curve above room temperature. For the simple copolymers at 30°C, SAXS reveals a microphase separated structure which increases in spacing, then disappears in the 60-70°C range. With cooling, the microphase separated structure reappears readily for the CHDI-based copolymer, while its reappearance shows a hysteresis resulting from rate effects for the other copolymers.

14. SUBJECT TERMS
Polyurethanes, Polyethylenes, Elastomers, Hydroxy Polyethylenes, Block Copolymers, Chemical Resistance

15. NUMBER OF PAGES
31

16. PRICE CODE

17. SECURITY CLASSIFICATION OF REPORT	**18. SECURITY CLASSIFICATION OF THIS PAGE**	**19. SECURITY CLASSIFICATION OF ABSTRACT**	**20. LIMITATION OF ABSTRACT**
Unclassified	Unclassified	Unclassified	UL

NSN 7540-01-280-5500

Standard Form 298 (Rev. 2-89)
Prescribed by ANSI Std. Z39-18
298-102

INTRODUCTION

Low molecular weight hydroxy terminated polyethylene (HTPE, Mitsubishi Kasei America, Inc.) is one of the most inert polyols which can be used to prepare high molecular weight polyurethanes and other block copolymers. The inertness of the soft segment contributes to an increased solvent resistance of the resulting polymers. The electrical properties, hydrolysis resistance and oxidative stability of polyethylene-based polyurethanes compared to other polyurethane elastomers makes them useful in many commercial applications[1]. Block copolymers with non-hydrogen bonding soft phases are also useful as model materials in which the importance of chemical and morphological features in determining the properties of the polymers can be studied.

Several groups have studied the chemistry[2] and properties[3,4] of hydroxy terminated polyethylene from other sources. The study of hydroxy terminated polybutadiene (HTPBD) is also relevant to this research, since the HTPE used is prepared from HTPBD by complete hydrogenation.

Preliminary reports about the properties of HTPE and polyurethane elastomers prepared from it have appeared[5,6]. This paper will include more complete results and discussions of the chemical structure of the polyol, the synthesis of polyurethane copolymers from the polyol and common diisocyanates and the synthesis of block copolymers, immersion experiments in which the solvent resistance of the polymers was evaluated, thermal analysis including dynamic mechanical analysis and results of combined X-ray - DSC experiments on the polyurethane samples.

EXPERIMENTAL

Characterization of HTPE

Gel permeation chromatography was performed on the HTPE in toluene at 35°C using a Waters chromatography system equipped with a R401 refractive index detector. A Jordi column oven was used to maintain constant temperature. Two Waters Ultrastyragel^{R} columns, a 500 A° and a 1000 A°, were connected in series and used for the analysis.

Vapor phase osmometry was performed using a Hitachi-Perkin-Elmer 115 Molecular Weight apparatus calibrated with benzil at 55°C using toluene as the solvent.

IR experiments were run on a Perkin-Elmer 1740 Infrared Fourier Transform Spectrometer in the ATR mode.

The Raman spectrum of the HTPE was obtained with a Spex FTR/IR FT-Raman spectrometer using an exciting line of 1064 nanometers. The waxy HTPE contained in a glass vial was placed in the beam of the instrument. One hundred scans were collected and the resolution of the spectrum was 4 cm^{-1}.

NMR experiments, both ^{1}H AND ^{13}C were performed on a Varian XL200 in deuterated benzene.

Polymer Synthesis

The chemical structures of the starting polyol and diisocyanates are shown in Figure 1. The polyurethane copolymers were prepared by mixing polyol preheated to 120°C with a 10 % excess (in equivalents) of diisocyanate at ambient temperature in a polyethylene beaker. The mixture was degassed under vacuum for about one minute and then poured into a stainless steel mold which had been treated with mold release. The samples were cured for two hours at 120°C, then cooled and removed from the mold. In the case of aliphatic diisocyanates, dibutyltin dilaurate was sometimes required as a catalyst. A bubble free sample using the methylene bis(4-phenylisocyanate) (MDI) could not be obtained by this technique, but with the addition of dilute HCl, the reaction was slowed so that the reacting polymer mixture could be poured into the mold.

The block copolymers were prepared by heating the HTPE, the toluene diisocyanate (TDI, a mixture of 80 % 2,4- and 20% 2,6- isomers), the 1,4-butanediol(BD) and in some cases a BD - trimethylolpropane (TMP) mixture separately to 120°C. First, the TDI was added to the HTPE in a disposeable beaker and thoroughly mixed and then the preheated chain extender or chain extender mixture was added and thoroughly mixed. The mixture was degassed under vacuum for 30 to 60 seconds, poured into a steel mold, which had been coated with mold release and preheated, and cured for 16 hours at 120°C.

Polyurethane Characterization

The solvent resistance of the polyurethanes was studied by immersing disks of one inch in diameter and 0.050 inches thick in a liquid of interest at approximately 22°C. The samples were removed from the jars, blotted dry and weighed at regular intervals, more often at the beginning of the experiment and less often as the experiment progresses. When the weight of the sample plus sorbed liquid reached a constant value, the experiment was ended.

Thermal analysis was carried out on a Perkin Elmer System 7 thermal analysis system. Low temperature transitions were determined on a DSC-7 equipped for cryogenic operation and chilled with liquid nitrogen. The sample chamber was purged with ultra-high purity helium, while the glovebox was purged with ultra-high purity nitrogen. Samples weighing between 10 and 15 mg were placed in standard crimped aluminum pans, chilled to -120°C, then heated from -120°C to 25°C at 20°/minute. Each sample was cycled twice, and the values reported are the average values for two runs.

Above-ambient transitions were studied using a DSC-7 equipped with an intercooler. The sample chamber and the glovebox were purged with ultra-high purity nitrogen. Samples weighing between 10 and 15 mg were encapsulated in stainless steel sample containers sealed with Viton o-rings. Samples were chilled to 0°C, heated at 20°/minute to 100°C, then cooled to 0°C at 100°/minute. The cycle was repeated and values are reported for both the first and second runs.

Annealing experiments were carried out on the HTPE and one of the TDI-HTPE copolymers by placing the samples (encapsulated in stainless steel sample pans sealed with o-rings) in the DSC cell, heating from 0°C to 40°C (35°C for the copolymer) and holding for 30 minutes, cooling to 0°C, scanning at 20°C/min to 100°C, cooling to 50°C,(45°C) holding for 30 minutes, cooling to 0°C, scanning to 100°C again and repeating at 10° intervals until the transitions occurred below the annealing temperature (about 90°C).

The Bashore-Rebound and Shore A Hardness were measured using ASTM methods D 2632 and D 2240 respectively.

Tensile properties were measured using ASTM method D638 Type V.

Dynamic mechanical analysis was performed using a Rheometrics RDS-7700. Samples were cut to 13x64 mm and were 1.3-1.5 mm thick. The temperature was increased at 2°C/min from -110°C to 150°C or higher with a strain setting of 0.496 % and a frequency of 6.28 radians per second.

Thermomechanical analysis was performed using a Perkin-Elmer Thermomechanical Analyzer TMS-1 with a Perkin-Elmer UU-1 temperature program controller. Samples were 1.3-1.5 mm thick. The weight used on the TMA probe was 20 g. The heating rate was 20°C/min. Samples were heated in a helium atmosphere from -100°C to the softening point of the sample or to a maximum of 270°C.

Polyethylene-based urethane elastomers were studied at elevated temperatures using both small and wide angle X-ray scattering at the SUNY beamline at National Synchrotron Light Source, Brookhaven National Laboratory, Upton, NY. The same apparatus was used for both types of experiments, changing the working distance between the specimen and the detector in order to shift between the small- and the wide-angle experiments. Supplementary SAXS data sets for the determination of the electron density variance were obtained through use of a Kratky camera employing infinite-slit optics and a conventional X-ray generator. On both instruments, the same wavelength of 0.154 nm was used. The synchrotron experimental setup is particularly adaptable, because of the short time in which a pattern may be obtained, for studying kinetic effects[9] and annealing effects[10] involving the multiphase microstructure of segmented polyurethanes. On the other hand, the Kratky camera was valuable for the determination of density variance, since it was set up to span a wider angular range. As will be shown, this is a matter of importance for the density variance determination.

Details of the experimental setup have been published[7-10], while the theoretical methodology used to analyze the small-angle X-ray scattering (SAXS) data is fully described elsewhere[9-11]. One parameter measured by the SAXS experiment is the electron density variance, measured by the Porod invariant method. The electron density variance $\langle(\Delta\rho_e)^2\rangle$ is defined as the average squared fluctuation in electron density ρ_e from its mean value $\rho_{e,ave}$ for the polymer. Such a quantity is determined by the Porod Invariant method, which involves an integral Q of the SAXS intensity over all scattering space, defined by:

$$Q = \int_0^{+\infty} q^p \, I(q) \, dq, \tag{1}$$

where the intensity I(q) is a function of the variable q, given by

$$q = (4\pi/\lambda) \sin\theta,$$

in which λ is the wavelength and θ is half the scattering angle 2θ. In equation (1), the power p is 1 for an infinite-slit instrument, such as the Kratky camera, and 2 for the pinhole optics used with synchrotron instrument. From the Porod Invariant Q and with the use of suitable calibration and instruments factors[11] one may calculate the electron density variance $\langle(\Delta\rho_e)^2\rangle$. Since no instrument provides intensity data at either endpoint of 0 and ∞ of the integration, extrapolations at both ends are required to complete the integration. In this regard the Porod Invariant values obtained with the Kratky camera are preferred since, in these experiments, the Kratky camera spanned a wider range of q values, reducing the dependence upon such extrapolations. In practice, the variance results from the Kratky camera are reported in absolute terms, while the variance results from the synchrotron heating experiments are reported in relative terms, as the ratio of the current value to its value at the start of the heating experiment.

For an ideal two-phase system with sharp boundaries the electron density variance is given by:

$$\langle(\Delta\rho_e)^2\rangle = \phi_1 \; \phi_2 \; (\rho_1 - \rho_2)^2 \qquad (3)$$

where ϕ_i and ρ_i are the volume fraction and the electron density of the ith phase. Thus as a sample goes from microphase separated, as at ambient temperature, to homogeneous (complete phase mixing), as at above an upper phase separation temperature, where $\rho_1 = \rho_2$, the variance will go from finite to zero.

RESULTS AND DISCUSSION

Chemical Characterization of HTPE

The HTPE is a waxy solid which liquifies at about 85°C. Gel permeation chromatography on the polyethylene was performed in toluene and the molecular weights were determined relative to polystyrene. The chromatogram exhibits a Gaussian distribution of molecular weights. The number average molecular weight was 3160, the weight average was 8640 and the polydispersity 2.74. Vapor phase osmometry yielded a number average molecular weight of 3340, consistent with the GPC result. The equivalent weight, as determined by end group titration, was 1230. Dividing the number average molecular weight by the titrated value results in a functionality of 2.6 for this sample. The manufacturer states that the polyol has a functionality of 1.5-3.0, but on average is approximately equal to 2.3.

The HTPE is prepared by hydrogenation of hydroxy functionalized polybutadiene (HTPBD). No double bonds are present in the Raman spectrum absorbing at 1650 cm^{-1}. The Raman spectrum (see Fig. 2) indicates a high concentration of methyl groups, which absorb at 2900 cm^{-1}. These result from the hydrogenation of vinyl groups, which are present to the extent of 20 % of the repeat units in domestic $HTPBD_2$ (PolyBD R45M, Elf Atochem). Vinyl content as high as 55 % has been reported[12].

Functionalities for HTPBD have been reported between 1.9 and 2.6. Several studies of functionality for polyols prepared from butadiene, which also most often yields polyols whose functionality usually exceeds 2.0, have been published[13-15].

The hydrogenation of HTPBD has been studied, but in that work, only 65 percent saturation was achieved[3]. A comparison of the properties of polyurethanes prepared from HTPBD with HTPE will be discussed later.

The ^{1}H and ^{13}C spectra for HTPE are shown in Fig. 3. From ^{1}H NMR, the estimated concentration of vinyl groups in the HTPBD from which the HTPE is made is slightly over 20% the total repeat units, equivalent on average to a vinyl group every eighteenth carbon atom. The proton NMR integration calculates to a vinyl group about every sixteenth carbon atom. This means that between 20 and 25 % of the monomer repeat units are vinyl groups and that the HTPBD used to prepare the HTPE is very similar in structure to Poly BD R45M (formerly Arco R45M). Another interesting feature of both the proton and carbon NMR is the presence of more than one peak in the region where carbon atoms and protons associated with alcohols occur. These peaks occur at 3.5-3.6 and 4.36 in the proton spectrum. There is more than one type of alcohol present, a primary bonded to a straight chain sequence and a primary on a carbon atom adjacent to a branch point[16]. The peak at 4.36 is probably due to an alcoholic proton since that HTPE analysis indicates a very low water content of less than 0.1 % and the NMR was run in deuterated benzene, a solvent with no exchangeable protons. There are also two peaks in the ^{13}C spectrum at 62.3 and 64.4 ppm, which indicates that there are two types of carbon atoms bonded to the hydroxy group. Both carbons are bonded to primary alcohol groups, but one of them has an ethyl branch on the carbon alpha to the alcohol carbon. The chemical structure of the HTPE is shown in Fig. 1.

Characterization of the Polyurethanes

Elastomeric polyurethane copolymers were prepared from HTPE and several common diisocyanates, including TDI, HDI (hexamethylene diisocyanate), MDI, H_{12}MDI [methylene bis(4-cyclohexylisocyanate) or hydrogenated MDI], IPDI (isophorone diisocyanate) and CHDI (trans-1,4- diisocyanatocyclohexane). All are translucent. Block copolymers were also prepared with toluene diisocyante and 1,4-butanediol or a mixture of 1,4-butanediol and trimethylolpropane, a cross-linker for the hard block. The compositions of the samples are listed in Table 1. Trimethylolpropane was used in small amounts to study the effect of a cross-linker in the hard block on the solvent resistance. The soft block is cross-linked because the functionality of HTPE is greater than two. These polyurethanes, prepared as described in the experimental section, are opaque. Cuve, Pascault, Boiteux and Seytre[4] reported block copolymers from TDI, BD and HTPE which were transparent. These polymers were prepared in solution and from a HTPE with an $F_n = 1.8$. In the present work, copolymers prepared from TDI and a HTPE with $F_n = 1.8$ (not described in detail here) were also clear. They were prepared neat. All the polymers prepared with HTPE with an F_n of 2.6 were translucent or opaque. Block copolymers prepared with CHDI, BD and HTPE with $F_n = 1.8$ were also translucent when prepared neat. Cuve, Pascault and Boiteux[20] also report the preparation of transparent polyethylene-based polyurethanes prepared in solution with MDI, BD and HTPE with $F_n = 1.8$ and hard sgement contents up to 40 weight %. The polymers with more than 40 % hard segment were opaque. The HTPE which was used by Cuve was reported to have an ethyl group on average bonded to every third carbon atom in the main chain. Transparency has also been reported for a HTPBD-based block copolymer with the molar composition 2.1 TDI-1 HTPBD-1.2 BD[12]. Samples with higher hard segment compositions were translucent or opaque. The HTPBD used in these polymers had 55 % vinyl monomer content.

Considerations of Transparency

New transparent materials with favorable solvent resistance are essential materials for certain technological developments. The polyurethanes discussed here are either transparent or not based on a combination of factors, including low weight percent hard segment, low crystallinity or good matches in the refractive indices of the hard and soft segments or the phase mixed regions. It appears that higher ethyl contents in the HTPE and higher vinyl contents in the HTPBD contribute to the transparency. The effect of branching on the morphology of polyethylene will be discussed in connection with thermal analysis later. The retention of transparency in the end use of the elastomer must be studied. Stress, exposure to solvents and thermal treatments could result in changes in the polymeric material which could cause reductions in transparency. Sometimes, use of thinner films can result in acceptable levels of translucency for many applications.

Infrared Spectroscopy

The infrared spectrum for 1.1 CHDI-1 HTPE is shown in Fig. 4A and the carbonyl regions of the infrared spectra for three polymers are shown in Fig. 4B. The peaks at 1728-1737 cm^{-1} are the free carbonyl frequencies, those at 1683 to 1709 cm^{-1} are the hydrogen-bonded carbonyl frequencies and those at 1711 to 1721 cm^{-1} represent weaker hydrogen bonding interactions. Note that the 1.1 CHDI-1 HTPE exhibits considerably more hydrogen bonding than the others and that the hydrogen bonding is stronger. This means that the diisocyanate portion of that sample is very strongly associated because there are no hydrogen bonding sites in the HTPE. The diisocyantes hydrogen bond only to each other, suggesting that the CHDI is more insoluble in the HTPE than the other diisocyanates or that crystallization of the the CHDI moiety drives the separation of the urethane formed with the CHDI. Thus, the polyurethane prepared with CHDI has more polyethylene character and is more chemically resistant.

The infrared spectra for the copolymers provides useful information about differences in morphology. The carbonyl region of the polyurethane copolymer prepared with CHDI is significantly different from that region for the other copolymers studied, exhibiting a sharp carbonyl - hydrogen bonded peak at 1683 cm^{-1}. Based on peak heights of the three carbonyl peaks in the IR, 63 % of the total carbonyl groups belong to the hydrogen-bonded peak. The data are listed in Table 2. The other copolymers behave differently. For example, the copolymer prepared from MDI also exhibits three peaks in the carbonyl region, but they are broad and overlapping. The carbonyl - hydrogen bonded peak at 1709 cm^{-1} represents 37% of the total for that sample. The relative positions of the hydrogen bonded peak for the two samples indicates that the hydrogen bonding in the CHDI-based polymer is stronger. This suggests that the CHDI-based polyurethane is better phase segregated and that the HTPE phase of the polymer has more polyethylene character. It is more like a block copolymer, but with very short blocks and is slightly more resistant to 1,5-dichloropentane, which will be discussed later.

Shore A Hardness and Bashore Resilience

All of the polymers prepared from HTPE exhibit Shore A Hardness values between 80 and 92. These are typical values for softer elastomers, while harder elastomers must be measured using the Shore D Hardness tester. The polymers exhibit Bashore Rebound Resilience between 27 and 54, which would be acceptible for certain applications, but not for others. Polyurethanes with low Bashore

Rebound values (optimally below 20) have been studied for shock absorption applications[17]. Many resilient elastomeric rubber compounds have values in the 70 to 80 range.

Tensile Strength

Stress-strain measurements were performed on four samples of copolymers prepared from HTPE and diisocyanates TDI, CHDI, H_{12}MDI and HDI. As noted earlier, these polymers are chemically crosslinked because the HTPE has more than two hydroxy groups on average per molecule. Hence they behave in a manner similar to block copolymers which have physical crosslinks. The tensile strength values, 22-31 MPa, and elongation values, 427-456%, are comparable to those of polyurethane elastomers of the block copolymer type. There is an upturn in the stress-strain curve which might be caused by additional stress crystallization of the HTPE in the polymer chain. Stress-strain measurements on the block copolymers have not been performed. In a recent study, phase segregated polyurethanes prepared from hydrogenated polybutadiene exhibited a 49% improvement in tensile strength and a 53% improvement in elongation over polyurethanes prepared from the same unsaturated HTPBD[3].

Immersion in Chemical Agent Simulants

The results of immersion in 1,5-dichloropentane and diisopropyl methyl phosphonate are shown in Table 3. Equilibrium was reached in approximately 24 hours for the copolymers and at somewhat longer times for the block copolymers. Note that the samples prepared with CHDI sorbed the smallest amount of both liquids. Polyethylene exhibits gains of less than 4% under similar conditions, but several standard elastomers will gain 2 to 300% and then fall apart under these conditions[18]. The block copolymers exhibit equilibruium weight uptakes in 1,5-dichloropentane of 27 to 33% and are in the same range as the copolymers. A sample prepared from 1.1 H_{12}MDI-1 HTPBD(R45M) gained 500% in 1,5-dichloropentane. In general, samples prepared from HTPE gain significantly less 1,5-dichloropentane than most polyurethanes examined[19].

Differential Scanning Calorimetry

Pure HTPE exhibits a T_g of -40°C, which is increased four to seven degrees in the polyurethanes. The T_g's of the block copolymers were examined by dynamic mechanical analysis and will be discussed later.

Above room temperature, the HTPE shows transitions over the range of 38°C to about 90°C, illustrated in Fig. 5B. The transition at 38°C at first looks like a T_g, but a more careful analysis of the entire transition region requires a different interpretation. The DSC transitions in this region collectively are very much like the diffuse endotherm reported for another hydrogenated HTPBD[3]. The transition which appears on the second run is a single broad endotherm, also shown in Fig. 5B.

All the copolymers show T_g's at about -30 to -40°C. Above room temperature, most of the samples exhibit two broad overlapping endotherms between 38°C and 85°C on the initial scan. The polymer based on CHDI shows only one endotherm at about 60°C. On the second scan, a single endothermic transition appears. The annealing experiments described in the experimental section revealed at least two melting transitions in the HTPE and 1.1 TDI-1 HTPE. It was not possible to obtain a single sharp crystalline transition by annealing. In general, the transitions were broad. There was no evidence of a T_g above room temperature. In some cases, there was evidence of crystallization between the transitions. Examples of the DSC scans after annealing for the 1.1 TDI-1 HTPE have appeared. The figure is incorrectly referenced in the preprint[6] and shows the annealing behavior for the copolymer, not for HTPE itself. DSC scans on representative block copolymers from 0 to 100°C produced only a single peak and little or no evidence of a T_g for the hard segment. The transition data for all samples are summarized in Table 1.

There have been reports of the properties of other HTPE's and polyurethanes prepared from them. In one study the properties of HTPBD were compared to the properties of hydrogenated HTPBD which was 65 % hydrogenated. Arco R45M (now PolyBD R45M from Elf Atochem) was used, which is reported to be 20 % vinyl, 20 % cis and 60 % trans. The R45M exhibits a T_g at -81°C and in copolymers prepared with TDI and BD, the T_g is raised slightly[9] to -72°C. Other second order transitions at 24°C and 72°C are attributed to the hard segment. When HTPBD is hydrogenated to the extent of 65 % (HTPE-65), the T_g increases to -70 and two additional transitions are present: a diffuse endotherm from -50 to 25°C and another endotherm at 39°C. The polyurethanes prepared from HTPE-65 with TDI and BD show Tg's of -65 to -72°C. The diffuse endotherm occurs over a slightly lower temperature range and then T_g's at 35-40°C and 65-75°C, which are attributed to hard segment groups of different lengths.

The HTPBD from Japan Synthetic Rubber[12] has a vinyl content of 55 %, trans content of 35 % and cis content of 10 % (the T_g is -65°C). In the block copolymers prepared with TDI and BD, the soft segment T_g is raised to -56°C. A second order transition at 20°C and an endotherm at 55°C are attributed to the hard segment. It would be unusual to have a hard segment endotherm at this low temperature. The behavior of this polyol on hydrogenation has not been reported.

Cuve, Pascault and Boiteux report the thermal properties of a polyurethane[4] prepared with the HTPE (F_n = 1.8, M_n = 2100) from Nippon Soda at a mole ratio of 4 TDI-1 HTPE-3 BD. The soft segment T_g is -35°C and the hard segment exhibits a T_g of 34°C on the first DSC scan and elevation of the T_g to 94°C on the second scan. It was also reported[20] that a copolymer prepared with the HTPE (F_n = 1.8) and MDI is completely amorphous when polymerized in solution and shows no hard segment T_g or other transitons above room temperature.

The presence of ethyl groups in any HTPE may result in a somewhat stiffer polyurethane than is desireable for some applications. This is so because the main chain length is reduced for a given molecular weight by the formula weight of the ethyl groups present in side chains. This reduces the distance between hard segment phases and stiffens the polymer, provided that the phase mixing is low. It probably also reduces the crystalline character of the straight chain sequences, which could contribute to decreased stiffness in the final product.

The effect of methyl groups on the crystallinity of polyethylene has been studied[21]. With 60 methyl groups per 1000 carbon atoms, 20 % crystallinity has been reported and for 45 methyl groups per 1000, 48 % crystallinity. The number of ethyl groups for the HTPE used in the present study calculates to about 60, and so less than 20 % crystallinity would be expected in the HTPE, assuming that ethyl groups have a greater effect on reduction of crystallinity than methyl groups and also due to molecular weight effects and chain end defects. The number of ethyl groups in the HTPE from Nippon Soda is uncertain (compare Ref. 4 with Ref. 20), but if it is more than in that from Mitsubishi Kasei, then that could help to explain the transparency of the polyurethanes prepared in solution from it.

Thermomechanical analysis on the two component copolymers reveals final softening temperatures of 220 to 250°C typical of polyurethane elastomers containing cross-linking by covalent bonds. The dynamic mechanical behavior of the polymers at elevated temperatures will be discussed in the next section.

Dynamic Mechanical Analysis

All the copolymers except the CHDI-based copolymer exhibit only one discernable broad tan δ peak attributable to the T_g of HTPE. The tan δ maxima are very broad, as shown in Fig. 6A for 1.1 TDI-1 HTPE and in the data in Table 4. The CHDI-based copolymer shows a narrower tan δ peak for the T_g of HTPE. Above 40°C, a transition is discernable in the G" curve, which corresponds to the endothermic transitions present in the same temperature region in the DSC.

The block copolymer samples prepared from TDI exhibit a considerably narrower tan δ peak at about -25°C and another transition varying in temperature between 43°C and 47°C. Only one peak appears in the G" curve, at the lower temperature. The transition above room temperature is like that for the copolymers, due primarily to a melting-like process. Remember that a hard segment T_g was not identifiable in the DSC curve for three representative block copolymers and so the lack of a transition due to the hard segment T_g in the dynamic mechanical spectrum is not unexpected. Note also that the storage modulus (the upper curve) is nearly constant up to about 150°C, which indicates that short term use at that temperature mightbe possible.

Storage modulus values for the two component materials (see Fig. 6A and Table 5) compare well with values of 16-98 MPa for block copolymers recently studied[22]. Stiffness values here are useful only for relative comparisons of different samples using the same dynamic technique. The block copolymers vary considerably in their stiffness, depending on the weight percent hard segment and also the amount of cross-linker. The stiffness decreases with an increase in temperature from 20 to 25°C for all the samples in the table. In general, a wide range of stiffness can be achieved with these starting materials.

X-Ray Results

Five copolymers containing only the polyol and a diisocyanate, as indicated in Table 6, were studied by X-ray diffraction methods. In the wide angle patterns obtained as a function of temperature for the 1.1 CHDI-1 HTPE copolymer and summarized in Fig. 7A, only a broad amorphous halo was seen at all temperatures between 30 and 216°C. The maximum position of the amorphous halo shifted to lower scattering angles with increasing temperature, reflecting the general thermal expansion of the structure. The wide angle pattern indicates that the HTPE soft segment material, which predominates in the polymer in terms of mass, lacks short range order.

For comparison, the room temperature wide angle pattern of the unreacted HTPE resin (a waxy solid) is shown in Fig. 7B. Three crystalline peaks are evident, which may be identified with known polyethylene reflections: the monoclinic (001) peak at 19.5°, the orthorhombic (110) peak at 21.5°, and the orthorhombic (200) peak at 23.6°, superimposed on a quite strong amorphous halo. Thus two separate crystalline phases are present, along with appreciable amorphous content. It is postulated that the crystallization process in the neat HTPE resin accompanies a fractionation process, selecting molecules more suitable (based on linearity and/or molecular weight) for one or the other crystalline phase to form crystallites. The fact that such distinct crystalline reflections are present in the neat resin, but not in the urethane elastomer, is attributed to the restraint placed on the HTPE chains by the urethane polymerization, which prevents such fractionation. Nonetheless, crystallites do appear to form from the HTPE soft segments in the elastomers, albeit of notably smaller size and possible greater degree of imperfection. A typical set of SAXS patterns as a function of temperature is shown in Fig. 8 for the 1.1 TDI-1 HTPE. At 30, 40, and 50°C, as seen in Fig. 8, a SAXS maximum appeared. The maximum shifted to lower angle (higher repeat period) with increasing temperature, weakened at 60°C, then vanished at higher temperatures. Assuming the maximum is attributable to a lamellar repeating structure, such a lamellar spacing may be obtained from the position of the maximum in the Lorentz-corrected scattering pattern as recommended by Ophir and Wilkes[23]. The calculated repeat period was approximately 10 nm at 30°C. (The position of the maximum was found to be dependent upon temperature, but not upon the nature of the diisocyanate constituent of the polyurethane.) As the temperature was lowered from its maximum of 180°C, a hysteresis effect was observed (Fig. 9), in that the diffraction maximum did not reappear until 40°C was reached. At ascending temperatures, the microstructure, resulting from the microphase separation of the two molecular species, was at equilibrium. However, once a homogeneous melt was achieved above 60°C, reforming that microstructure as the temperature was reduced could be governed by a rate process which resulted in the observed hysteresis. The present work indicates that this hysteresis is common to all of the copolymers studied.

The microphase separation process may be quantitatively followed by use of the Porod invariant, a measure of the variance in electron density, resulting from the separation of the molecules into less- and more-dense microphases. Further information[11] is available on the methodology of determining the Porod Invariant, which involves a mathematical integration, after appropriate correction for background and diffuse scattering, over the SAXS intensity curve. Kratky camera SAXS patterns obtained at ambient temperature (not shown) were particularly useful in this regard, since a suitable method, based on a polyethylene standard, was available for determining the absolute intensity of the primary beam, which is necessary to interpret the results on an absolute basis. Such results are shown in Table 6, and are seen to fall in the range 0.7×10^{-3} to 1.2×10^{-3} (moles electrons/cm^3)^2. The differences in Table 6 could result from differences in the electron densities of the hard segment (diisocyanate) microphase, the fraction of hard segment material, thickness of a possible microphase boundary layer, and the degree of microphase separation. A detailed interpretation of the invariant values in terms of these microstructure parameters is outside the scope of the present investigation.

The Porod invariant method has also been applied to the SAXS data as a function of temperature and the results are shown in Fig. 10; experimental details of the experiment are given in Table 7. (Note that the synchrotron beam intensity was not calculated on an absolute basis; thus the Fig. 10 results are reported relative to the value of the electron density variance for the polymer at the start of the experiment. If needed, one may convert the relative data of Fig. 10 into absolute electron density variance values by reference to the Kratky camera data for the startifng polymers in Table 6.) At the time scale of the SAXS heating experiment, it is seen that the copolymers show pronounced hysteresis between the ascending temperature curve and its descending temperature counterpart. Evidently the process of resegregating the homogeneous melt into a microphase separated morphology is intrinsically slower than the reverse process of forming the homogeneous melt. For the CHDI-based HTPE copolymer, however, the hysteresis is less pronounced. Although the falling-temperature curve lags below the rising-temperature curve for this polymer in Fig. 10, and are separated at 60° and 50°, the data for the two curves rejoin below 40°, indicating that the microstructure is reversibly recovered, albeit after a delay resulting from the finite rate of the microphase separation kinetics. This is in agreement with results from the DSC experiments.

In this context, one notes that the disappearance of the microphase separated morphology at ascending temperatures near 60°C coincides roughly with the melting range of the HTPE oligomer. The high level of short-chain side branches would tend to limit the ability of the soft segment to crystallize; however, the HTPE oligomer used in this study existed as a semicrystalline waxy solid before reaction rather than as a liquid. Although the wide angle X-ray data failed to reveal the soft segment crystallinity, an aggregation into very small and defective crystallites could provide an enthalpic driving force for microphase separation below this temperature range.

CONCLUSIONS

HTPE-based polyurethanes can be readily prepared as copolymers or segmented copolymers from a wide variety of components. The preparation of polymers has not been fully explored here, since a true prepolymer step was not employed. The use of this HTPE in Reaction Injection Molding using a completely heated poly side (polyol tank, cylinder, hoses and mixhead) and viscosity modifiers for the HTPE is being explored1[9]. The copolymer and block copolymer polyurethanes prepared here exhibit useful mechanical properties, in part due to the high F_n (=2.6) of the HTPE, which results in cross-linking. So far, transparent polyurethane elastomers have only been obtained with the HTPE having an F_n = 1.8, but not an F_n = 2.6 upon which this research is based. Transparency is of interest because that property, combined with the superior solvent resistance of HTPE-based polyurethanes, suggests applications as flexible lens materials for which few good materials exist. Solvent resistance, measured by immersion tests with 1,5-dichloropentane, is superior to that of the customary polyether- and polyester-based polyurethane elastomers.

Infrared studies indicate association of urethane units even in the copolymers, with the highest degree occurring in the CHDI-based copolymer. However, it is not possible to specify the size of the urethane clusters and no hard segment transition can be detected by DSC. Although DSC indicates a broad endothermal region above 45°C in the polyurethanes due to melting of HTPE, low angle X-ray experiments reveal only an amorphous halo. This indicates that the short range order which is present in the HTPE before incorporation into the polyurethane is surpressed by the restraint imposed by the urethane linkage, clustering, and by the high degree of cross-linking resulting from F_n = 2.6.

Further research is needed to gain an improved understanding of the morphology and the effect of increasing the hard segment size. In addition, it is important to separate the contribution of cross-linking from that of urethane clustering by comparing polyurethanes prepared with the current HTPE and an analogous HTPE with $F_n = 1.8$.

ACKNOWLEDGMENTS

This research was sponsored by the U.S. Department of the Army and by the Department of Energy, #DEFG0286ER45237A009.

REFERENCES

(1) Mitsubishi Kasei America, Inc., 81 Main Street, White Plains, N.Y.

(2) W.S. Anderson, "Telechelic Polyethylene", Contemp. Top. Polym. Sci., v.4, W.J. Bailey and T. Tsuruta, eds., Plenum Press, N.Y., 1984, p.95.

(3) C.M. Brunette, S.L. Hsu, W.J. MacKnight and N.S. Schneider, "Structural and Mechanical Properties of Polybutadiene-Containing Polyurethanes", Polym. Eng. Sci. 21,163(1981).

(4) L. Cuve, J.-P. Pascault, G. Boiteux and G. Seytre, "Synthesis and Properties of Polyurethanes based on Polyolefin: 1. Rigid Polyurethanes and Amorphous Segmented Polyurethanes Prepared in Polar Solvents under Homogeneous Conditions", Polymer **32**, 343 (1991).

(5) C.A. Byrne and E.A. McHugh,"Hydroxy Terminated Polyethylene and Polyurethanes Prepared From It", Polymer Preprints **31**(2), 657 (1990).

(6) C.A. Byrne, C.R. Desper, N.S. Schneider, B. Chu and T. Gao, "Polyethylene-Based Polyurethane Block Copolymers", Polymer Preprints **34** (2), 602 (1993).

(7) B. Chu, D. Wu, and C. Wu, "Kratky Block-Collimation Small-Angle X-Ray Diffractometer for Synchrotron Radiation", Rev. Sci. Instrum. **58**, 1158 (1987).

(8) D. Wu, "Synchrotron Small-Angle X-Ray Scattering of Ion-Containing Polymers", Ph.D. Thesis, SUNY at Stony Brook, Stony Brook, NY, 1990.

(9) B. Chu, T. Gao, Y. Li, J. Wang, C. R. Desper, and C. A. Byrne, "Microphase Separation Kinetics in Segmented Polyurethanes: Effects of Soft Segment Length and Structure", Macromolecules **25**, 5724 (1992).

(10)Y. Li, T. Gao, J. Liu, K. Linliu, C. R. Desper, and B. Chu, "Multiphase Structure of a Segmented Polyurethane: Effects of Temperature and Annealing", Macromolecules **25**, 7365 (1992).

(11)C. R. Desper, C.A. Byrne, B. Chu, and Y. Li, "Morphologu Studies of CHDI-Based Urethane Elastomers by Synchrotron X-Ray Diffraction", submitted to Macromolecules.

(12)C.M. Brunette, S.L. Hsu, M. Rossman, W.J. MacKnight and N.S. Schneider, "Thermal and Mechanical Properties of Linear Segmented Polyurethanes with Butadiene Soft Segments", Polymer Eng. Sci. **21**, 668(1981).

(13)J.N. Anderson, S.K. Baczek, H.E. Adams and L.E. Vescelius, "Functionality Distribution of Hydroxyl-Terminated Polybutadienes Using Gel Permeation Chromatography. I. The Method and Calibration Procedure", J. Appl.Polym. Sci. **19**, 2255 (1975).

(14)S.K. Baczek, J.N. Anderson and H.E. Adams, "Functionality Distribution of Hydroxyl-Terminated Polybutadienes Using Gel Permeation Chromatography. II. Measurements for Commercial Polymers, J. Appl. Polym. Sci. **19**, 2269-2277 (1975).

(15)Ramey, Kermit, "Characterization of R-45M, AFRPL-TR-74-64.

(16)Y. Tanaka, "Recent Advances in Structural Characterization of Elastomers", Rubber Chem. Tech. **64**, 325 (1991).

(17)C.A. Byrne and W.X. Zukas, "Studies of Polymers for Shock Absorption Applications", Adv. Ureth. Sci. Tech. **12**, 105 (1993).

(18)A.F. Wilde, "Standard Rubbers for Chemical Defense Research Volume II: MTL Immersion Tests with Decontaminants and Simulants", MTL TR 89-48.

(19)S.W.Wong, B. Meng, C.A.Byrne and T.F.Kenney,Jr., to be published.

(20)L. Cuve, J.-P. Pascault and G. Boiteux, "Synthesis and properties of polyurethanes based on polyolefin: 2. Semicrystalline segmented polyurethanes prepared under heterogeneous or homogeneous synthesis conditions", Polymer **33**, 3957 (1992).

(21)S.L. Aggarwal, in J. Brandrup and E.H. Immergut, eds., Polymer Handbook, 2nd ed., Wiley, N.Y., 1975, p. V-19, "Properties of Polyethylene".

(22)J.W.Dieter and C.A.Byrne, "Aliphatic Polyurethanes with High Performance Properties", Polym. Eng. Sci. **27**, 673 (1987).

(23)Z. Ophir and G.L. Wilkes, "SAXS Analysis of a Linear Polyester and a Linear Polyether Urethane - Interfacial Thickness Determination", J. Polym. Sci,Polym. Phys. Ed. **18**, 1469(1980).

APPENDIX

HYDROXY COMPONENTS

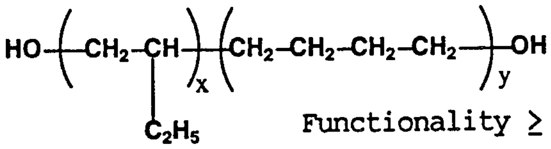

$HO-(CH_2-CH(C_2H_5))_x-(CH_2-CH_2-CH_2-CH_2)_y-OH$

Functionality ≥ 2

$HO-CH_2-CH_2-CH_2-CH_2-OH$

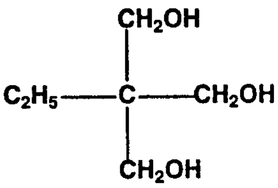

DIISOCYANATES

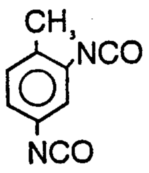

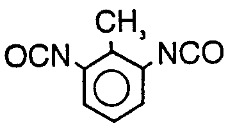

$OCN(CH_2)_6NCO$

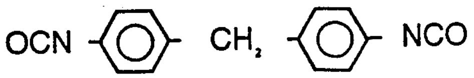

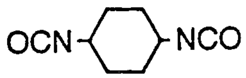

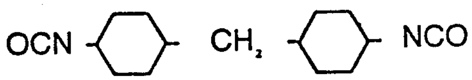

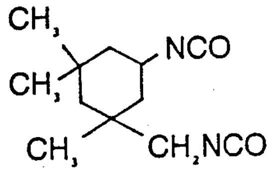

DIBUTYLTIN DILAURATE

Fig. 1. The Chemical Structures of the Polyurethane Components.

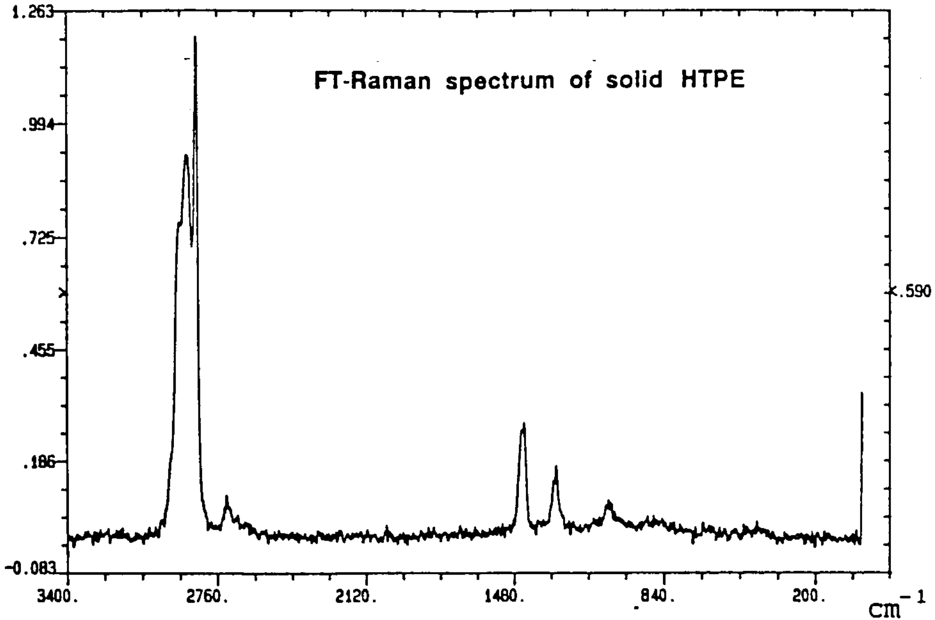

Fig. 2. The FT-Raman spectrum of HTPE.

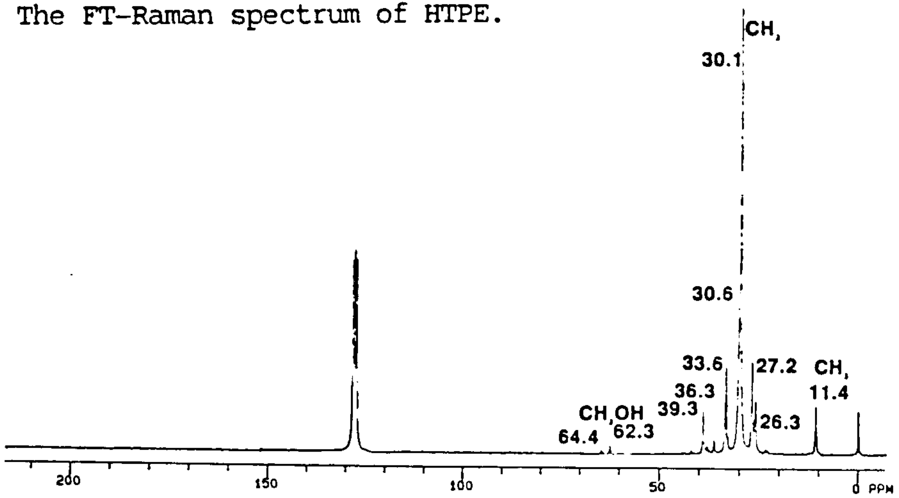

Fig. 3A. The ^{1}H NMR of HTPE in Benzene-d_6/$CDCl_3$.

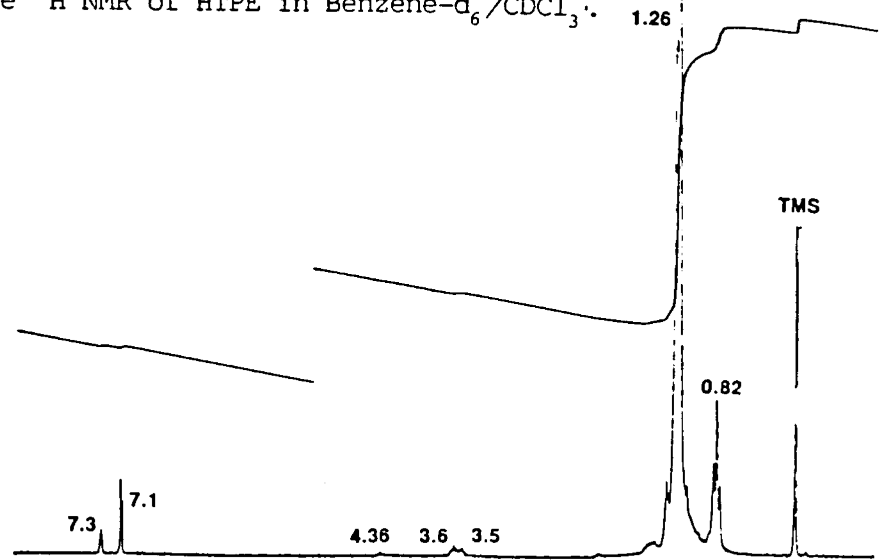

Fig. 3B. The ^{13}C NMR of HTPE in Benzene-d_6.

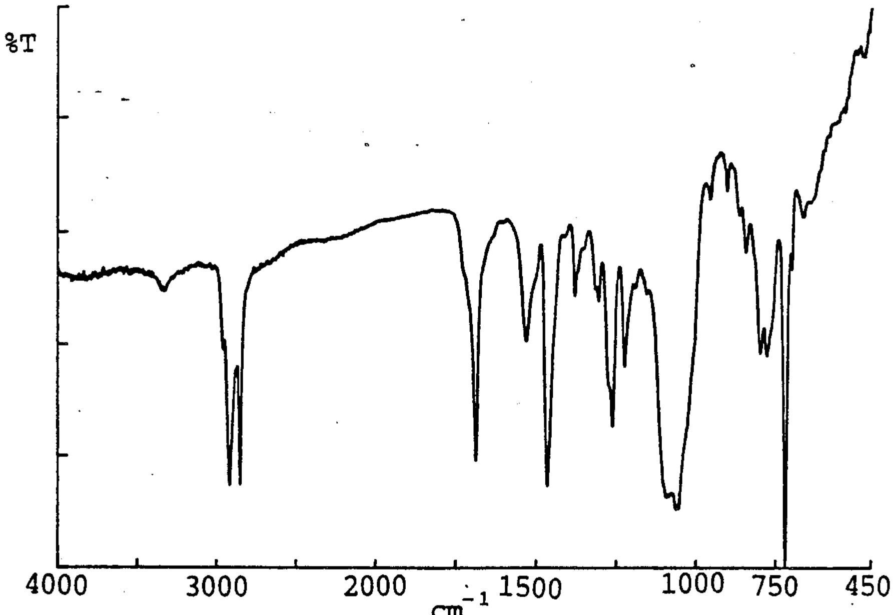

Fig. 4A. The FT-IR spectrum of 1.1 CHDI-1 HTPE.

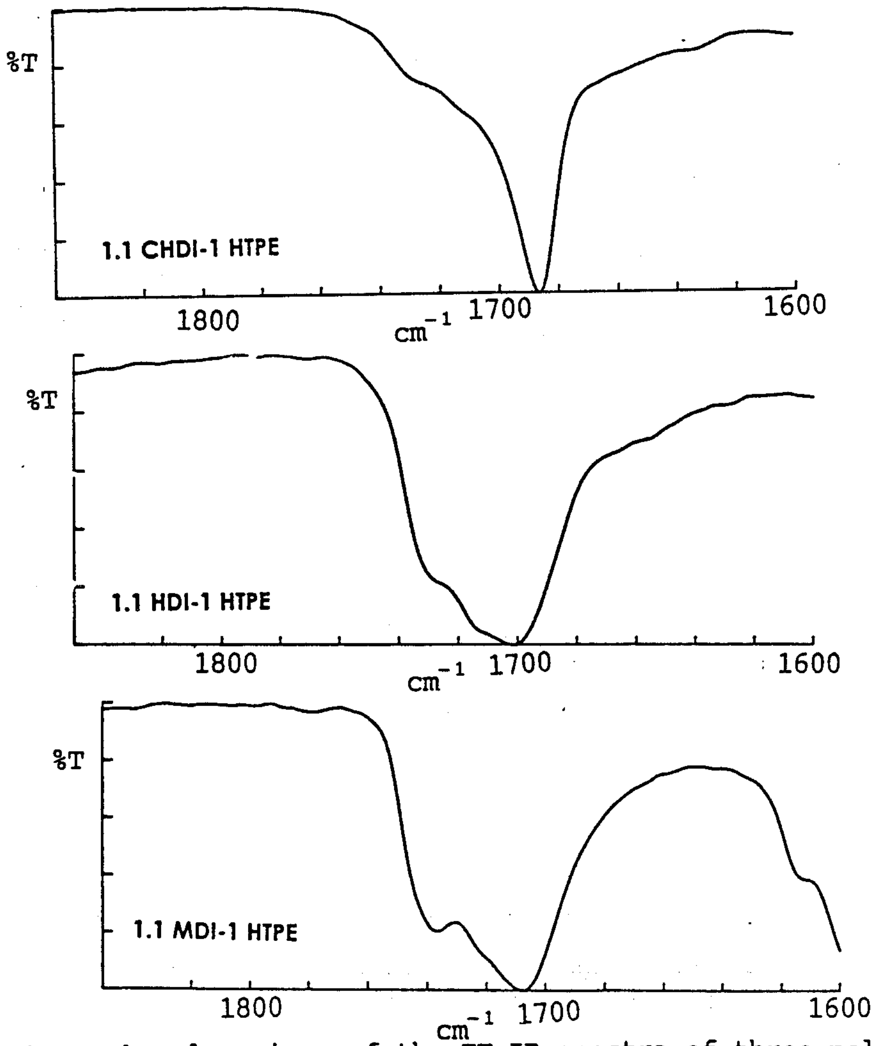

Fig. 4B. The carbonyl regions of the FT-IR spectra of three polyurethanes.

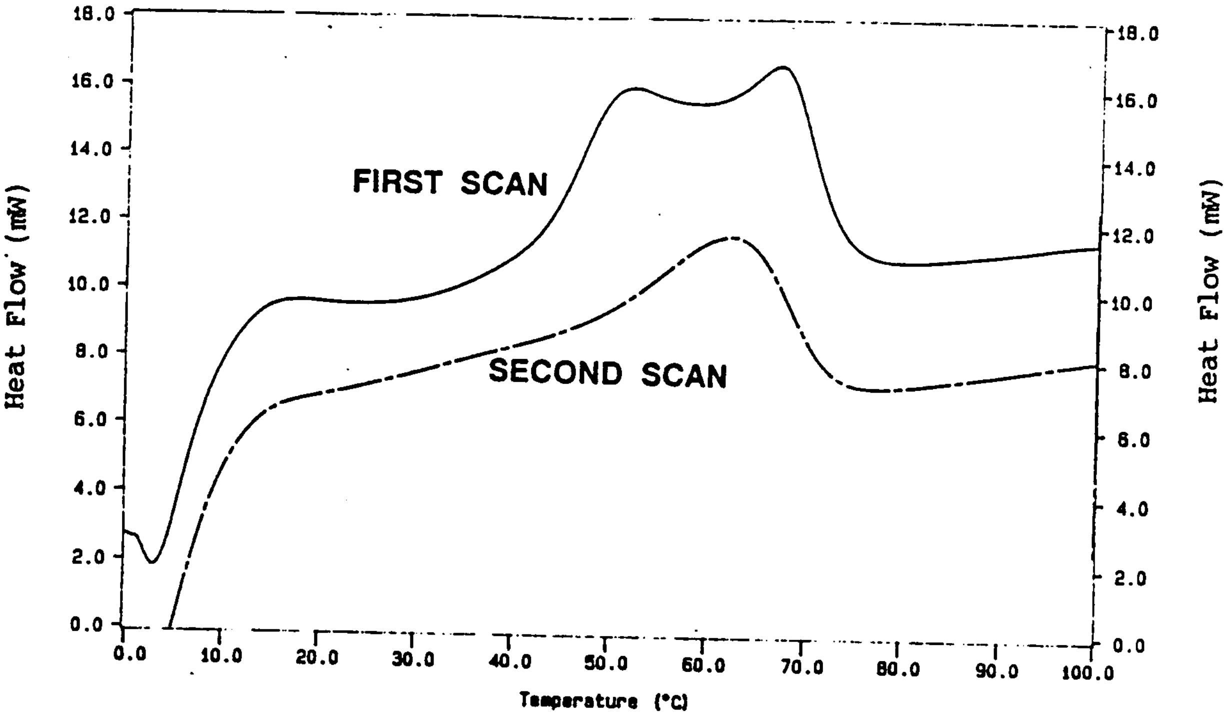

Fig. 5A. DSC Scans of 1.1 TDI-1 HTPE. Scan Rate = 20°C/min. Sample Size = 12.15mg.

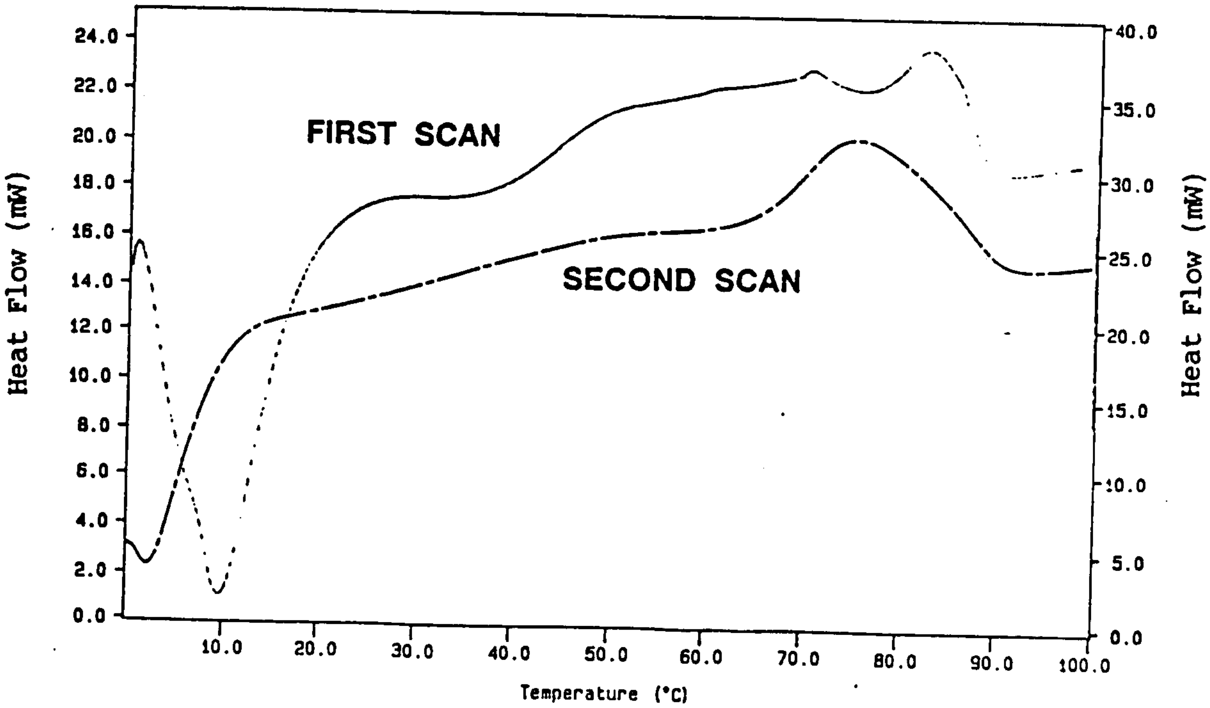

Fig. 5B. DSC Scans of HTPE. Scan Rate = 20°C/min. Sample size = 13.42mg.

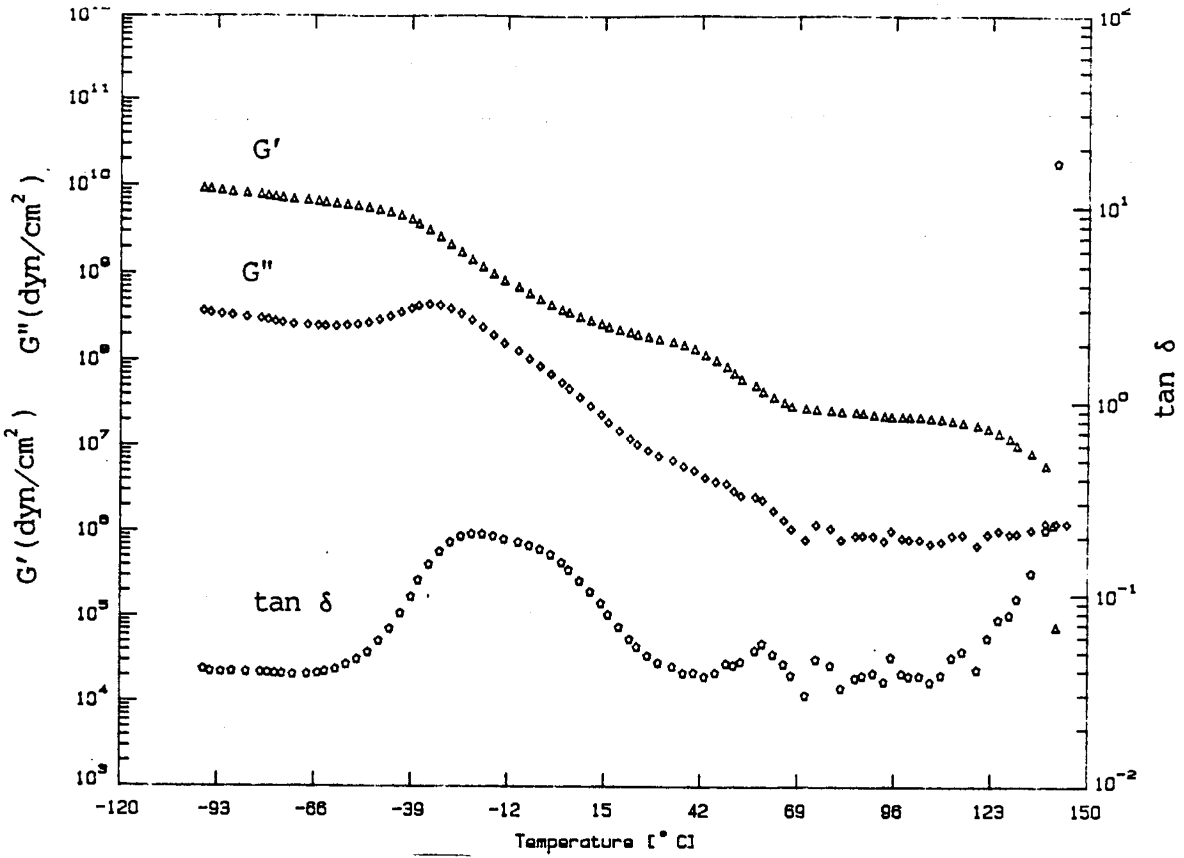

Fig. 6A. The Dynamic Mechanical Spectrum of 1.1 TDI-1 HTPE. Scan rate = 2°C/min. Strain setting = 0.496%. Frequency = 6.28rad/s.

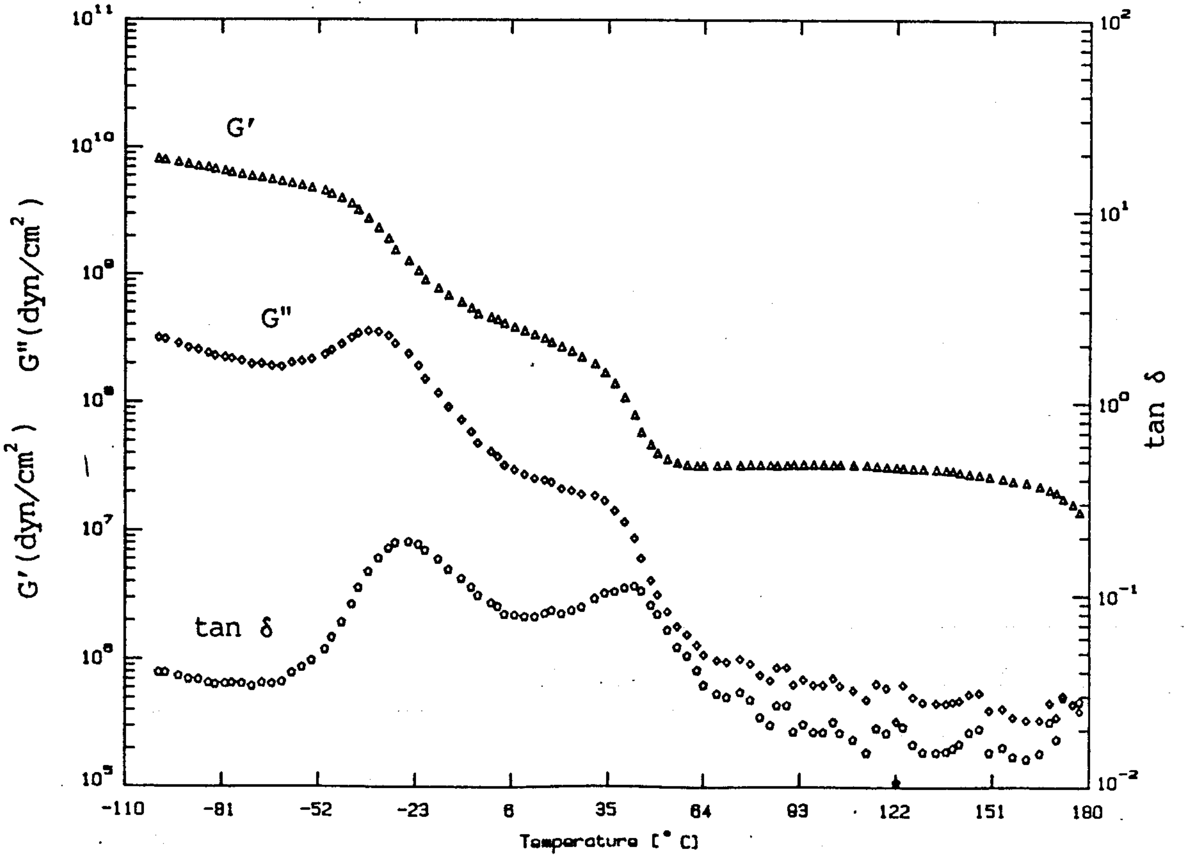

Fig. 6B. The Dynamic Mechanical Spectrum of 2.2 TDI-1 HTPE-0.9375 BD-0.0625 TMP. Scan rate = 2°C/min. Strain setting = 0.496%. Frequency = 6.28rad/s.

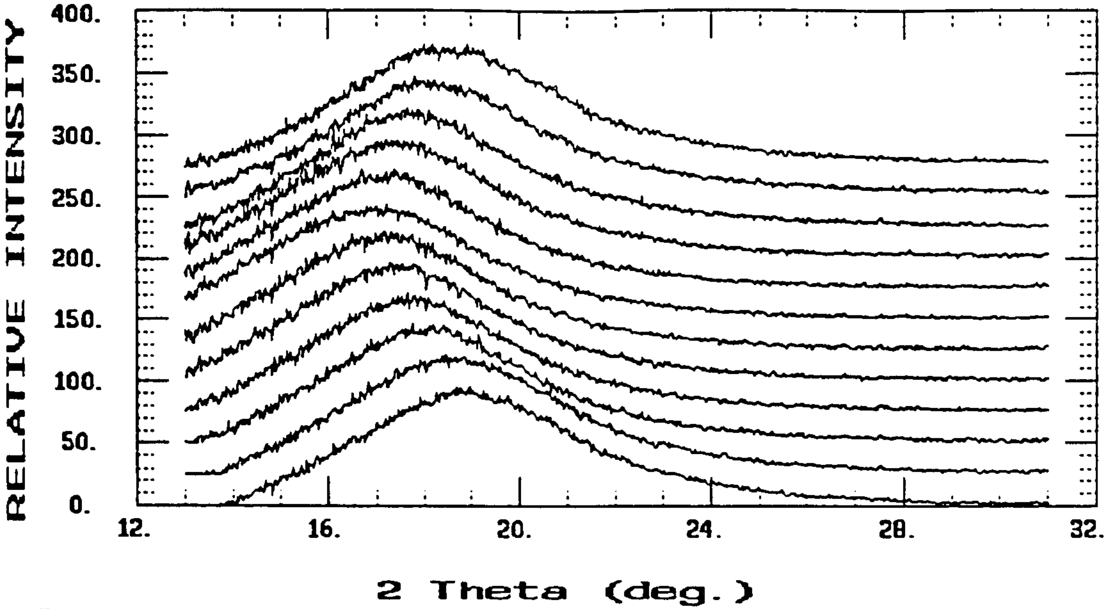

Fig. 7A. Wide angle X-ray diffraction patterns as a function of temperature for 1.1 CHDI-1 HTPE. Temperatures, beginning with the lowest curve: 30, 52, 76, 112, 151, 185, 216, 186, 155, 114, 53, 43°C. For clarity, a number of patterns at intervening temperatures have been omitted. The X-ray wavelength is 0.154nm for all experiments reported here.

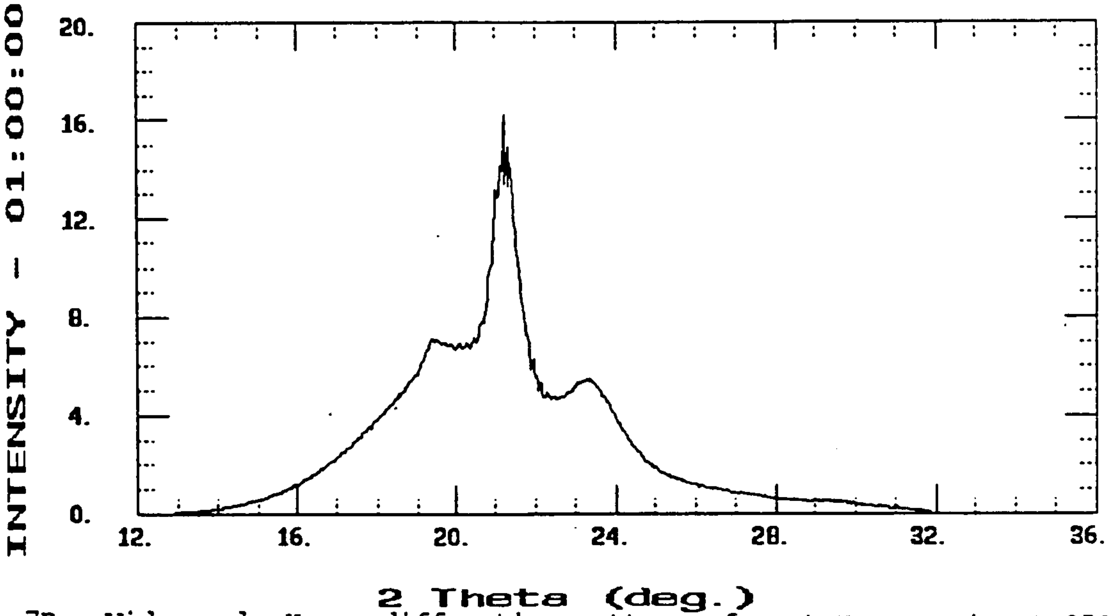

Fig. 7B. Wide angle X-ray diffraction pattern of neat HTPE resin at 25°C.

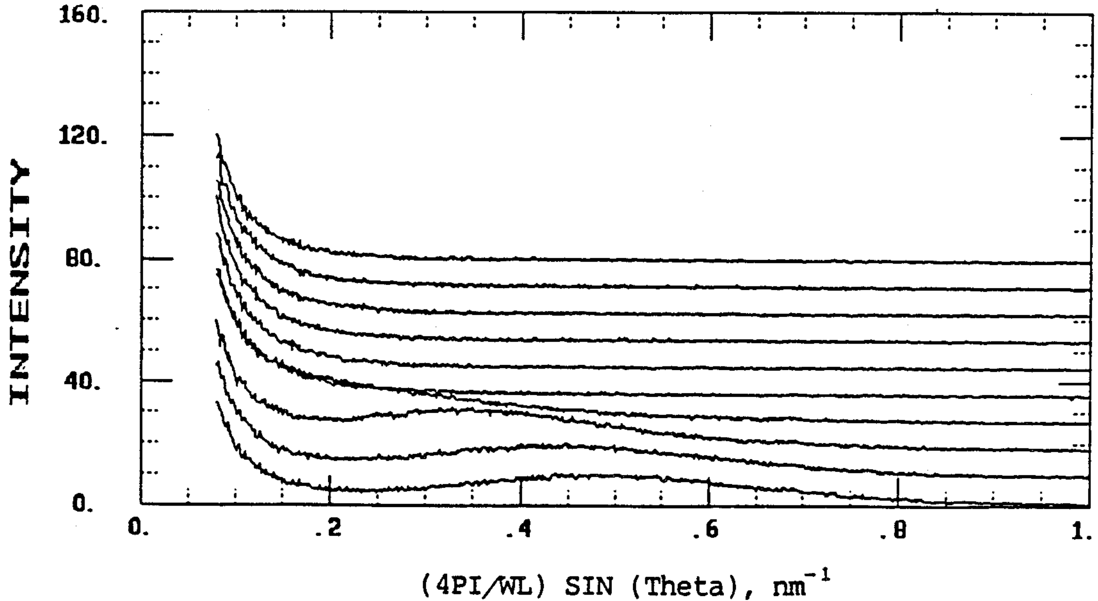

Fig. 8. Small angle X-ray scattering patterns as a function of temperature for 1.1 TDI-1 HTPE. Ascending temperatures, beginning with the lowest curve: 30, 40, 50, 60, 70, 80, 100, 120, 150, 180°C.

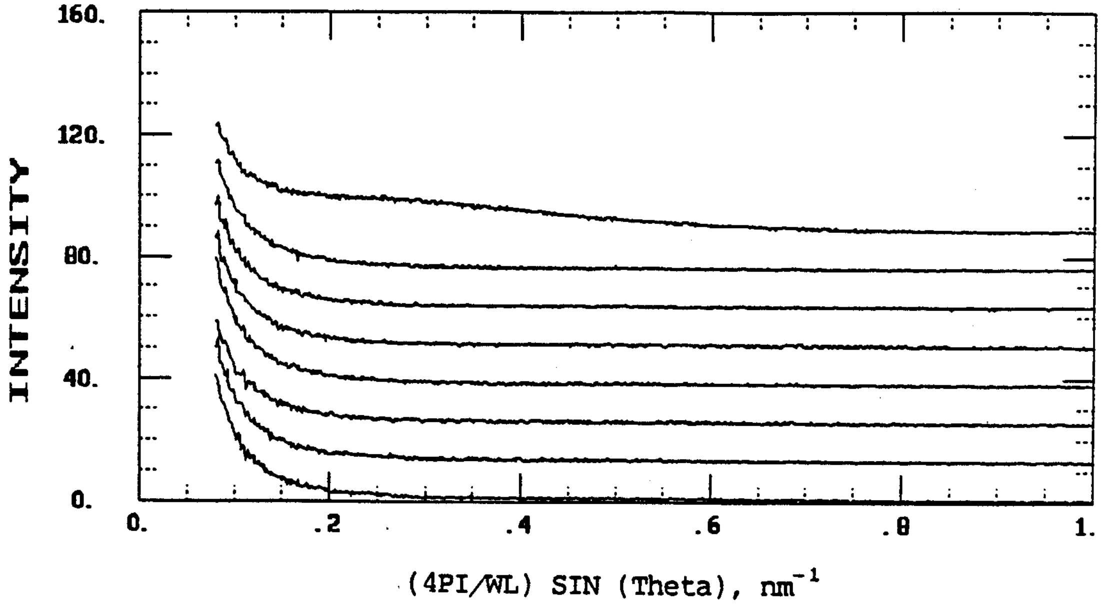

Fig. 9. Small angle X-ray scattering patterns as a function of temperature for 1.1 TDI-1 HTPE. Descending temperatures, beginning with the lowest curve: 180, 150, 120, 80, 70, 60, 50, 40°C.

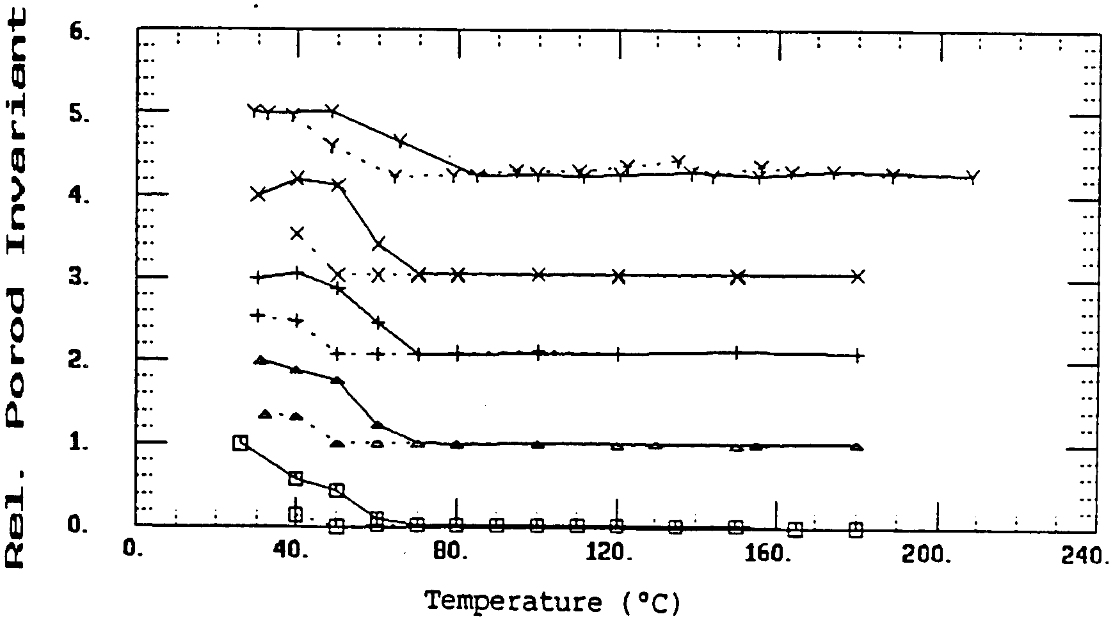

Fig. 10. Relative values of the Porod invariant for SAXS heating experiments for five HTPE-based copolymers. Solid lines: ascending temperatures; dashed lines: descending temperatures. The diisocyanate component of the elastomer, beginning with the lowest curve: MDI, HDI, H_{12}MDI, TDI and CHDI. Curves for successive elastomers are offset by 1.0 for clarity. Each curve represents the ratio of invariant to the starting invariant value; thus all curves begin at the value 1.0 plus the offset.

Table 1. List of Samples

Sample Composition (equivalents)	Weight% Hard Segment	DSC Transitions(°C)	
		T_g a)	Peak
HTPE	–	-40	43, 83
Second Scan		–	75
1.1 TDI-1 HTPE	7.2	-33	52, 67
Second Scan		–	62
1.1 H_{12}MDI-1 HTPE	10.5	-36	50, 63
Second Scan		–	60
1.1 HDI-1 HTPE	7.0	-30	52, 68
Second Scan		–	64
1.1 CHDI-1 HTPE	6.9	-34	60
Second Scan		–	59
1.1 IPDI-1 HTPE	9.0	a)	
1.1 MDI-1 HTPE	10.0	-40	52, 66
Second Scan			62
2.1 TDI-1 HTPE-0.5BD-0.5TMP	15.6	a)	
2.1 TDI-1 HTPE-0.75BD-0.25TMP	15.6	a)	
2.1 TDI-1 HTPE-0.875BD-0.125TMP	15.6	a)	
2.1 TDI-1 HTPE-1.0TMP	15.6	a)	
2.2 TDI-1 HTPE-0.9375BD-0.0625TMP	16.1	a)	52
Second Scan			55
3.2 TDI-1 HTPE-2.0BD	22.9	a)	53
Second Scan			54
3.2 TDI-1 HTPE-1.5BD-0.5TMP	22.8	a)	
3.2 TDI-1 HTPE-1.75BD-0.25TMP	22.9	a)	
3.2 TDI-1 HTPE-1.875BD-0.125TMP	22.9	a)	
3.2 TDI-1 HTPE-2TMP	22.8	a)	
3.3 TDI-1 HTPE-2.0BD	23.5	a)	
3.3 TDI-1 HTPE-1.875BD-0.125TMP	23.5	a)	
3.3 TDI-1 HTPE-2TMP	23.5	a)	
4.2 TDI-1 HTPE-2.5BD-0.5TMP	28.9	a)	
4.2 TDI-1 HTPE-2.75BD-0.25TMP	28.9	a)	
4.2 TDI-1 HTPE-2.875BD-0.125TMP	28.9	a)	53
Second Scan			53
4.2 TDI-1 HTPE-3TMP	28.9	a)	
4.4 TDI-1 HTPE-2.8125BD-0.1875TMP	29.6	a)	

a) No data.

Table 2. Analysis of the Carbonyl Region

Sample Composition (Equivalents)	Wavelength of Peak (cm^{-1})	Percent of Total Carbonyl[a]
1.1 CHDI-1 HTPE	1683	62.8
	1711	22.5
	1728	14.7
1.1 HDI-1 HTPE	1703	36.4
	1714	34.7
	1728	28.9
1.1 MDI-1 HTPE	1709	36.9
	1721	32.9
	1737	30.2

a) Based on relative peak heights.

Table 3. Maximum Weight Gain on Immersion

Sample Composition (equivalents)	1,5-Dichloro-pentane(%)	Diisopropyl-methyl Phosphonate(%)
1.1 TDI-1 HTPE	31	23
1.1 H_{12}MDI-1 HTPE	36	17
1.1 HDI-1 HTPE	31	18
1.1 CHDI-1 HTPE	21	12
1.1 MDI-1 HTPE	31	28
2.1 TDI-1 HTPE-1TMP	33	a)
2.2 TDI-1 HTPE-0.9375BD-0.0625TMP	33	a)
3.2 TDI-1 HTPE-2BD	31	a)
3.3 TDI-1 HTPE-2BD	27	a)
4.2 TDI-1 HTPE-2.875BD-0.125TMP	32	a)
1.1 H_{12}MDI-1 HTPBD[b]	500	a)

a) No data.

b) HTPBD is PolyBD R45M from Elf Atochem.

Table 4. Dynamic Mechanical Analysis Results

Sample Composition (equivalents)	Tan Delta Peak (°C)[a]
1.1 TDI-1 HTPE	-16 to -22
1.1 H_{12}MDI-1 HTPE	-9 to -22
1.1 HDI-1 HTPE	-21 to -23
1.1 CHDI-1 HTPE	-24, 57
1.1 IPDI-1 HTPE	-13 to -19
1.1 MDI-1 HTPE	-16 to -22
2.1 TDI-1 HTPE-0.75BD-0.25TMP	-25, 43
2.2 TDI-1 HTPE-0.9375BD-0.0625TMP	-25, 43
3.2 TDI-1 HTPE-2.0BD	-25, 42 to 45
4.2 TDI-1 HTPE-2.875BD-0.125TMP	-26, 45 to 47

a) See text for discussion of transitions.

Table 5. Storage Modulus from Dynamic Mechanical Spectra

Sample Composition (equivalents)	G′ at 20°C(MPa)	G′ at 25°C(MPa)
1.1 2,4-TDI-1 HTPE	15.4	13.9
1.1 TDI-1 HTPE[a]	21.0	18.9
1.1 HDI-1 HTPE	15.3	14.6
1.1 2,6-TDI-1 HTPE	7.8	6.6
1.1 H_{12}MDI-1 HTPE	18.4	16.1
1.1 IPDI-1 HTPE	15.0	13.7
1.1 CHDI-1 HTPE	25.9	24.6
1.1 MDI-1 HTPE	16.4	14.7
2.1 TDI-1 HTPE-0.5 BD-0.5 TMP	21.7	18.7
2.1 TDI-1 HTPE-0.75 BD-0.25 TMP	23.0	18.9
2.2 TDI-1 HTPE-0.9375 BD-0.0625 TMP	27.1	23.5
3.15TDI-1 HTPE-1.5 BD-0.5 TMP	30.4	27.3
3.15TDI-1 HTPE-1.75 BD-0.25 TMP	45.3	38.2
3.3 TDI-1 HTPE-1.875 BD-0.125 TMP	47.1	39.3
4.2 TDI-1 HTPE-2.75 BD-0.25 TMP	34.0	31.0

a) TDI is a mixture of 80% 2,4-isomer and 20% 2,6-isomer unless otherwise specified.

Table 6. Copolymer Electron Density Variance values from SAXS Kratky Camera Data - Infinite Slit Optics

Polymer Constituents (equivalents)	Temperature (°C)	Electron Fraction Hard Segment	Electron Density Variance (moles electrons/cm^3)^2
1.1TDI-1 HTPE	19	0.066	0.72×10^{-3}
1.1H_{12}MDI-1 HTPE	22	0.100	0.73×10^{-3}
1.1HDI-1 HTPE	21	0.066	0.84×10^{-3}
1.1CHDI-1 HTPE	21	0.064	1.16×10^{-3}
1.1MDI-1 HTPE	22	0.092	0.93×10^{-3}

Table 7. Experimental Details of SAXS Heating Experiments Synchrotron Source Data - Pinhole Optics[a)]

Polymer Constituents (equivalents)	Number of Patterns	Time / Pattern (Seconds)[b)]
1.1TDI-1 HTPE	17	400
1.1H_{12}MDI-1 HTPE	19	400
1.1HDI-1 HTPE	18	300
1.1MDI-1 HTPE	26	300

[a)] Data Range for all Diffuse Intensity Determinations: $q = 0.80$ to $0.90\ nm^{-1}$. Data Range for all Porod Invariant Integrals: $q = 0.08$ to $0.90\ nm^{-1}$.

[b)] Between patterns, approximately 120 seconds elapsed while changing temperature.

DISTRIBUTION LIST

No. of Copies	To
1	Office of the Under Secretary of Defense for Research and Engineering, The Pentagon, Washington, DC 20301
	Director, U.S. Army Research Laboratory, 2800 Powder Mill Road, Adelphi, MD 20783-1197
1	ATTN: AMSRL-OP-SD-TP, Technical Publishing Branch
1	AMSRL-OP-SD-TA, Records Management
1	AMSRL-OP-SD-TL, Technical Library
1	AMSRL-MO-IF, R. Huang
3	AMSRL-MO-IF, M. Carr
	Commander, Defense Technical Information Center, Cameron Station, Building 5, 5010 Duke Street, Alexandria, VA 23304-6145
2	ATTN: DTIC-FDAC
1	MIA/CINDAS, Purdue University, 2595 Yeager Road, West Lafayette, IN 47905
	Commander, Army Research Office, P.O. Box 12211, Research Triangle Park, NC 27709-2211
1	ATTN: Information Processing Office
	Commander, U.S. Army Materiel Command, 5001 Eisenhower Avenue, Alexandria, VA 22333
1	ATTN: AMCSCI
3	AMCMI-IS-A
	Commander, U.S. Army Materiel Systems Analysis Activity, Aberdeen Proving Ground, MD 21005
1	ATTN: AMXSY-MP, H. Cohen
	Commander, U.S. Army Missile Command, Redstone Arsenal, AL 35809
1	ATTN: AMSMI-RD-CS-R/Doc
	Commander, U.S. Army Armament, Munitions and Chemical Command, Dover, NJ 07801
1	ATTN: Technical Library
	Commander, U.S. Army Natick Research, Development and Engineering Center Natick, MA 01760-5010
1	ATTN: SATNC-MI, Technical Library
1	SATNC-AI
	Commander, U.S. Army Satellite Communications Agency, Fort Monmouth, NJ 07703
1	ATTN: Technical Document Center
	Commander, U.S. Army Tank-Automotive Command, Warren, MI 48397-5000
1	ATTN: AMSTA-ZSK
1	AMSTA-TSL, Technical Library
1	AMSTA-SF
	President, Airborne, Electronics and Special Warfare Board, Fort Bragg, NC 28307
1	ATTN: Library

No. of Copies — To

Director, U.S. Army Research Laboratory, Weapons Technology, Aberdeen Proving Ground, MD 21005-5066
1 ATTN: AMSRL-WT
2 Technical Library

Commander, Dugway Proving Ground, UT 84022
1 ATTN: Technical Library, Technical Information Division

Commander, U.S. Army Research Laboratory, 2800 Powder Mill Road, Adelphi, MD 20783
1 ATTN: AMSRL-SS

Director, Benet Weapons Laboratory, LCWSL, USA AMCCOM, Watervliet, NY 12189
1 ATTN: AMSMC-LCB-TL
1 AMSMC-LCB-R
1 AMSMC-LCB-RM
1 AMSMC-LCB-RP

Commander, U.S. Army Foreign Science and Technology Center, 220 7th Street, N.E., Charlottesville, VA 22901-5396
3 ATTN: AIFRTC, Applied Technologies Branch, Gerald Schlesinger

Commander, U.S. Army Aeromedical Research Unit, P.O. Box 577, Fort Rucker, AL 36360
1 ATTN: Technical Library

U.S. Army Aviation Training Library, Fort Rucker, AL 36360
1 ATTN: Building 5906-5907

Commander, U.S. Army Agency for Aviation Safety, Fort Rucker, AL 3636
1 ATTN: Technical Library

Commander, Clarke Engineer School Library, 3202 Nebraska Ave., N., Fort Leonard Wood, MO 65473-5000
1 ATTN: Library

Commander, U.S. Army Engineer Waterways Experiment Station, P.O. Box 631, Vicksburg, MS 39180
1 ATTN: Research Center Library

Commandant, U.S. Army Quartermaster School, Fort Lee, VA 23801
1 ATTN: Quartermaster School Library

Naval Research Laboratory, Washington, DC 20375
1 ATTN: Code 6384

Chief of Naval Research, Arlington, VA 22217
1 ATTN: Code 471

Commander, U.S. Air Force Wright Research and Development Center, Wright-Patterson Air Force Base, OH 45433-6523
1 ATTN: WRDC/MLLP, M. Forney, Jr.
1 WRDC/MLBC, Mr. Stanley Schulman

No. of Copies	To
1	U.S. Department of Commerce, National Institute of Standards and Technology, Gaithersburg, MD 20899 ATTN: Stephen M Hsu, Chief, Ceramics Division, Institute for Materials Science and Engineering
1	Committee on Marine Structures, Marine Board, National Research Council, 2101 Constitution Avenue, N.W., Washington, DC 20418
1	Materials Sciences Corporation, Suite 250, 500 Office Center Drive, Fort Washington, PA 19034
1	Charles Stark Draper Laboratory, 555 Technology Square, Cambridge, MA 02139
1	General Dynamics, Convair Aerospace Division, P.O. Box 748, Fort Worth, TX 76101 ATTN: Mfg. Engineering Technical Library
1	Plastics Technical Evaluation Center, PLASTEC, ARDEC, Bldg. 355N, Picatinny Arsenal, NJ 07806-5000 ATTN: Harry Pebly
1	Department of the Army, Aerostructures Directorate, MS-266, U.S. Army Aviation R&T Activity - AVSCOM, Langley Research Center, Hampton, VA 23665-5225
1	NASA - Langley Research Center, Hampton, VA 23665-5255
1	U.S. Army Vehicle Propulsion Directorate, NASA Lewis Research Center, 2100 Brookpark Road, Cleveland, OH 44135-3191 ATTN: AMSRL-VP
1	Director, Defense Intelligence Agency, Washington, DC 20340-6053 ATTN: ODT-5A, Mr. Frank Jaeger
1	U.S. Army Communications and Electronics Command, Fort Monmouth, NJ 07703 ATTN: Technical Library
1	U.S. Army Research Laboratory, Electronic Power Sources Directorate, Fort Monmouth, NJ 07703 ATTN: Technical Library
1	Commander, U.S. Army Science and Technology Center-Far East, Unit #45015, APO AP 96343-0074 ATTN: AMXMI-J-OP
1	Commander, U.S. Army Science and Technology Center-Europe, Unit #25202, APO AE 09079 ATTN: AMXMI-E-CM
1	Commander, U.S. Belvoir Research, Development, and Engineering Center, Ft. Belvoir, VA 22060-5606 ATTN: SATBE-TY

No. of Copies	To
	Commander, U.S. Armament Research, Development, and Engineering Center, Picatinny Arsenal, NJ 07806-5000
1	ATTN: SMCAR-ASF
	Director, U.S. Army Research Laboratory, Watertown, MA 02172-0001
2	ATTN: AMSRL-OP-WT-IS, Technical Library
25	Authors